第 46 卷第 6 期 红外与激光工程 2017 年 6 月
Vol.46 No.6 Infrared and Laser Engineering Jun. 2017

Cylindrical optical micro-structure used in infrared laser protection

Sun Yanjun, Liu Shunrui, Wu Boqi, Wang Li, Wang Jun

(School of Photo-Electronic Engineering, Changchun University of Science and Technology, Changchun 130022, China)

Abstract: Laser protection is a technology of wide application. Aimed at the problem that strong absorption in visible wavelengths and equipment or operator injury caused by laser high-reflective film specular reflection exist in infrared laser protection technology, an infrared laser non-specular reflection optical micro-structure formed on optical material surface was presented. It had little effect on visible light transmission and large-angle scattering to 1 064 nm laser. Light track method was used to design double-side micro-cylindrical lens arrays with a dislocation construction. Array period T and curvature radius of lens units R should meet the condition: $0<T<R/2\sqrt{7}$. Virtual-Lab optical modeling software was applied for the simulation of designed micro-cylindrical lens arrays. The results is that, average transmittance rate of visible light drops 7%, which has little impact on practical result, and which can be made up by visible wavelengths fabrication antireflection coating; 1 064 nm infrared laser reflection is greater than 75%, divergence angle is greater than 30°. Fabrication experiment of micro-cylindrical lens arrays was finished by digital mask lithography technology, the test result was similar to simulation result. The conclusion is that, micro-cylindrical lens arrays can cause wide-angle scattering, which greatly reduces the single-directivity reflection echo energy of laser to achieve the purpose of laser protection.

Key words: infrared laser protection; optical micro-structure; cylindrical micro-lens
CLC number: TB133 **Document code:** A **DOI**: 10.3788/IRLA201746.0616001

柱面光学微结构用于红外激光防护研究

孙艳军,刘顺瑞,吴博奇,王 丽,王 君

(长春理工大学 光电工程学院,吉林 长春 130022)

摘 要:激光防护是一种可广泛应用的技术,论文针对目前红外激光防护技术中存在的可见光波段吸收强、镜面反射造成设备或人员损伤等问题,提出一种形成于光学窗口表面的红外激光非镜面反射光学微结构,具有对可见光透过率影响小,同时对 1 064 nm 红外激光大角度散射的功能,从而实现激光防护。文中采用光线追迹方法设计具有移位结构的双面微柱透镜阵列,阵列周期 T 与透镜单元曲率半径 R 之间需满足 $0<T<R/2\sqrt{7}$ 的关系。应用 Virtual-Lab 光学建模软件对设计的柱面微结构进行

收稿日期:2016-10-15; **修订日期**:2016-11-19

基金项目:国家自然科学基金(11474041)

作者简介:孙艳军(1978-),男,副教授,博士,主要从事光学微纳制造技术方面的研究。Email:custsun@126.com

模拟,模拟结果为:可见光平均透过率下降7%,对实用结果影响很小,并可以通过可见波段镀制增透膜进行弥补;1 064 nm 红外激光反射率约为75%,发散角大于30°。采用数字掩模光刻技术完成微柱透镜阵列实验,实验结果与模拟结果趋势相同,最终得出结论:微柱透镜阵列能实现大角度散射,能够极大降低激光单一方向反射回波能量,从而达到了激光防护的目的。

关键词: 红外激光防护; 光学微结构; 柱面微透镜

0 Introduction

Optical window of transmitting visible light, filtering or reducing infrared laser is used widely in laser protection field. Currently, there are two main methods of infrared laser protection; one way is to insert absorption elements of infrared laser to reduce laser light transmission. However, visible wavelength transmission losses much (over 20%) while filtering out infrared laser of visible light [1-2]. Another is to fabricate reflective coating on lens surface. The method also has some disadvantages. In case of high laser power of specular reflection, the reflected laser beam also harms human eye, skin, and other optical components. Therefore, exploring a laser protection technology which has little impact on visible light transmittance and scatters to infrared laser with large angle is very important [3-4]. That noted, the paper presents an infrared laser non-specular reflection optical micro-structure formed from optical window surface. It has little impact on visible light transmittance and avoids damage on laser vertical or inclined specular reflection to humans or instruments.

1 Cylindrical microstructure design

In order to achieve the purpose of normal incidence laser emitting at a certain angle, the shifting double cylindrical lens array was designed as in Fig.1[5]. We adopt ray tracing way, the lens unit is an axially symmetrical structure. Thus, we only discuss it in one direction. Wherein, L is any incident light, L_1, L_2, L_3 are respectively refractive light, reflected light and emergent light corresponding to L. Contour standard surface expression of cylindrical microstructure is:

$$z=\frac{cR^2}{1+\sqrt{1-(1+K)c^2R^2}} \tag{1}$$

In Eq. (1), c is the curvature, its value is the reciprocal of radius curvature R, $1/c=R=\pm b^2/a$, K is a quadric surface constant. If non specular reflection micro-structure design adopts cylindrical micro-lens as initial mathematical model, then k=0.

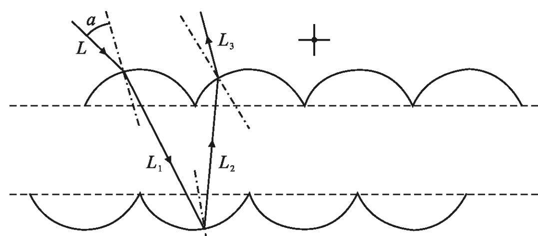

Fig.1 Optical pathway of double cylindrical micro-lens arrays with dislocation construction

Incidence angle at any point of cylindrical lens surface is 0°–90°. Incident light L reflects topper cylindrical lens array through lower cylindrical lens array to make emergent light and incident light into a certain angle. Refractive light emitted from point A has two special positions D and H, as shown in Fig.2(a)[6-7]. Two refractive lights through point D, H must meet conditions: $\angle ADB<\angle BDH$, $\angle AHF<\angle FHE$. Each angle is less than and greater than 0. When point A moves to A_1, $\angle A_1DB$ is in extreme position, as shown in Fig.2(b).

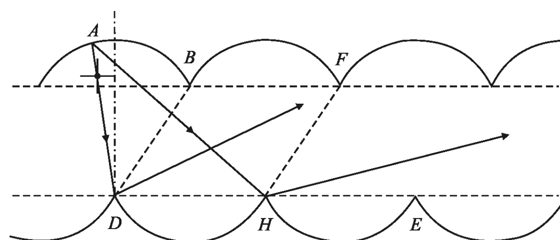

(a) Angular dependence

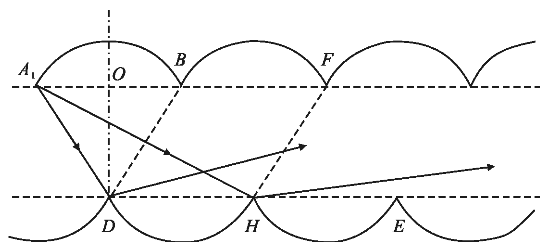

(b) Special position angular dependence

Fig.2 Ray propagation dependence

In the triangle A_1DO, sin $(\angle A_1DO)=T/2R$, then cylindrical lens $0<T<R$, thereby we obtain the relationship between cylindrical lens array period T and curvature radius of lens units R.

$$0<T<\frac{R}{2\sqrt{7}} \tag{2}$$

2 Function of cylindrical lens arrays

Single cylindrical lens thickness expression of cylinder unit structure as Fig.3 is:

$$d(x,y)=\sqrt{R^2-x^2}+h-\left[R-\sqrt{R^2-\left(\frac{T}{2}\pm x\right)^2}\right] \tag{3}$$

As $\sqrt{R^2-x^2}=\sqrt{R^2-\left(1-\frac{x^2}{R^2}\right)}\approx R\left(1-\frac{x^2}{2R^2}\right)$, Eq.(3) can be simplified as:

$$d(x,y)=R+h-\frac{T^2\pm 4Tx+8x^2}{8R} \tag{4}$$

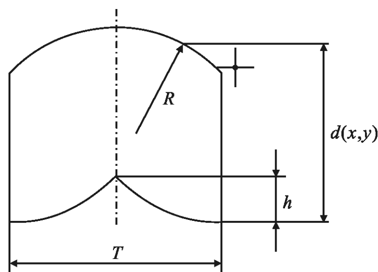

Fig.3 Unit structure of cylindrical micro-lens arrays

The function of single cylindrical lens transmission $t_0(x,y)$ by Eq.(4) is[8-9]:

$$t_0(x,y)=h_0\cdot\exp\left[j(n-1)k_0\left(\frac{T^2\pm 4Tx+8x^2}{8R}\right)\right] \tag{5}$$

Among them $h_0=\exp[-jk_0n(R+h)]$. The function of lens array transmission based on array theorem is:

$$t(x,y)=t_0(x,y)\cdot\sum_{n-1}^{N}\delta(x-\xi_n,y-\eta_n) \tag{6}$$

In formula (6), ξ_n,η_n are represented as any position in cylindrical lens[10]. Cylindrical lens array consists of n parallel lens units, each unit's period is T, we may deduce its transmittance:

$$t(x,y)=t_0(x,y)\cdot\sum_{n-1}^{N}\delta(x-nT)=t_0(x,y)\cdot\frac{1}{T}\mathrm{comb}\left(\frac{x}{T}\right) \tag{7}$$

We carry out Fourier transform on formula (7) to obtain spectral function of cylindrical lens array:

$$T(f_x,f_y)=F\{t_0(x,y)\}gF\left\{\frac{1}{T}\mathrm{comb}\left(\frac{x}{T}\right)\right\}=$$

$$T_0(f_x,f_y)g\mathrm{comb}\left(\frac{x}{T}\right) \tag{8}$$

Formula(8) indicates that cylindrical lens array is equal to the product of micro-lens unit spectrum and array spectrum arranging in the sameconfiguration. Non-reverse reflected cylindrical lens array power spectrum is:

$$|T(f_x,f_y)|^2=|T_0(f_x,f_y)|^2\cdot\left|\mathrm{comb}\left(\frac{x}{T}\right)\right|^2 \tag{9}$$

The light intensity distribution of micro-lens arrays accordingly is:

$$I(f_x,f_y)\propto|T(f_x,f_y)|^2 \tag{10}$$

3 Stimulation of cylindrical lens arrays

The paper is aimed at the requirements of 1 064 nm infrared laser protection and visible wavelengths. Combined with the boundary conditions of cylindrical lens array feature size and the difficulty of processing in further experiments, we set R=0.8 mm, T=0.18 mm, h=3 mm for cylindrical lens array unit, the upper and lower cylinder translocation is Δ=0.09 mm, as shown in Fig.3. We adopt Virtual-Lab optical modeling software. Then we set that the light source area is 0.4 mm×0.4 mm, the substrate material is QUARTZ glass; it is fabricated by 80-380 nm high permeability and 1 064 nm infrared laser high reflective coating.

3.1 Simulation of visible light transmission

532 nm wavelength surface light source is selected to vertically irradiate non-reverse reflected cylindrical

lens array. Figure 4 is diagram and curve of visible light intensity distribution. Non-reverse reflected cylindrical lens array has the effect of penetration and light equalization on visible light. The transmittance rate of QUARTZ glass substrate is about 95%, and the transmittance rate of cylindrical lens array is about 88% under 532 nm light. It decreases by 7% compared with that of QUARTZ glass in column-free lens array.

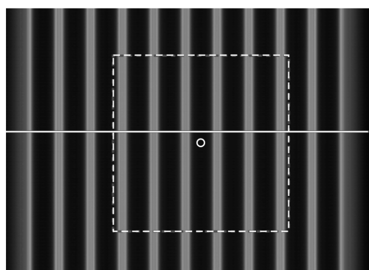

Fig.4 Energy distribution of 532 nm parallel light

3.2 Simulation of 1 064 nm laser wavelength reflection

The result of simulating 1 064 nm laser illuminant incident on the cylindrical lens arrays is shown in Fig.5.

(a) Simulation of parallel light vertical incidence

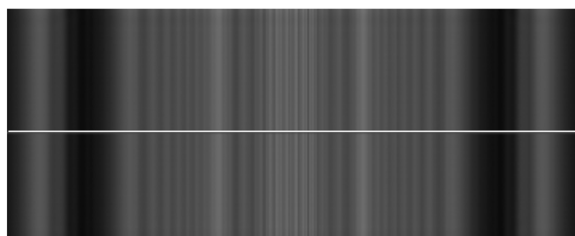

(b) Vertical incidence of parallel light energy distribution

Fig.5 Simulation graph of parallel light vertical incidence

From the simulation, light intensity is symmetrically distributed, the reflectance is about 76.32% ,the center echo rate is about 5% , the specular reflectance of QUARTZ glass in column-free lens array under 1 064 nm light is about 81.66% and cylindrical lens reflection echo decreased 76.66%. Thus, as laser incident on cylindrical lens array happens, reflected light energy spreads outward. It greatly decreases energy concentration, reduces the energy of laser reflection and plays function of laser protection.

Light intensity distribution on the receiving screen is about 0.4 −1.6 mm position. Illuminant, cylindrical lens array, receiving screen are right-angled triangle relationship. The incident light angle between emergentlight and vertical micro-lens array surface is α, and its value is:

$$\alpha=\arctan(l/L) \tag{11}$$

Wherein, the distance between light source and micro-structure is L=1 mm, L is the distance between light source to emergent light and receiving screen intersection. The angle α formed by right and left light source is 21.8° through calculation. Thus, the divergence angle of target echo is 43.6°. When light is incident on cylindrical lens array, the divergence angle of target echo will increase. It will reduce the energy of laser reverse echo.

From the previous analysis, the protection effect will be better with incident angle greater. So we simply discuss incident light in little angle, such as the following four cases: 5° 10°, 15°, 20°. Figure 6 is diffuse reflection of four incident angles.

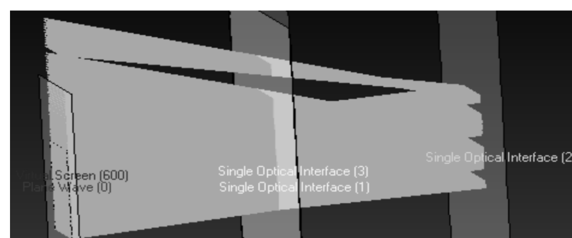

(a) Optical pathway of 5° incidence angle

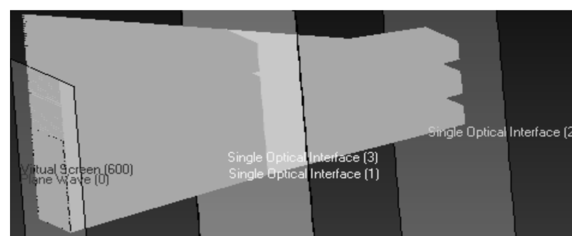

(b) Optical pathway of 10° incidence angle

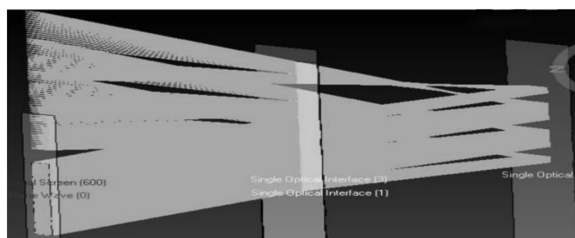

(c) Optical pathway of 15° incidence angle

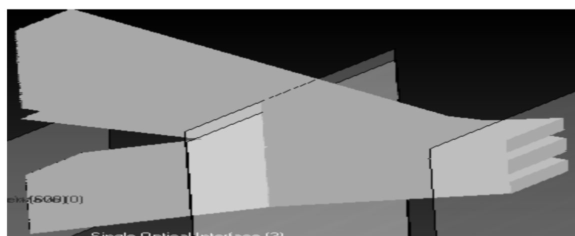

(d) Optical pathway of 20° incidence angle

Fig.6 Optical pathway of 5°, 10°, 15°, 20° incidence angle

Light intensity distribution curve shows that the angle α between emergent light and incident light has a certain range. Positive and negative angle indicate right and left direction of light source. By Eq.(11), we obtain α data shown in Tab.1.

Tab.1 Data table of light intensity distribution

Incident angle	Divergence angle	Angle of maximum intensity	Reflection boundary 1	Reflection boundary 2
5°	35.80°	13.50–7.97°	31.80	–4.00
10°	32.81°	26.57–17.80°	28.81	–4.00
15°	47.56°	37.86, 13.28°	50.69	3.13
20°	30.89°	38.66–33.28°	53.67	22.78

While 1 064 nm laser incident cylindrical lens array, the reflectance is approximately 75% and the divergence angle of target echo is greater than 30°. The maximum intensity area deviates from light source in a certain angle. It reduces the energy of laser backward echo to reach laser protection purpose.

4 Experiment research

In this experiment, lithography gray mask was generated utilizing Mat-lab software according to micro-structure parameters designed. We finished lithography experiment utilizing DS–2000/14G digital mask lithography machine, and photoresist micro-structure was fabricated on quartz substrate surface by development etc, shown in Fig.7.

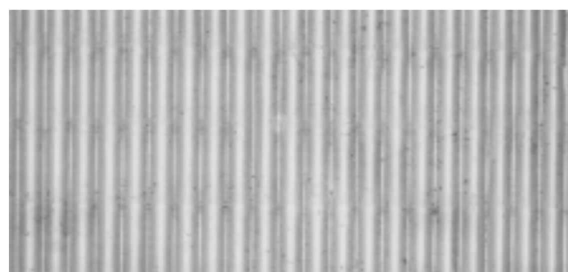

(a) Photoresist graphic structure

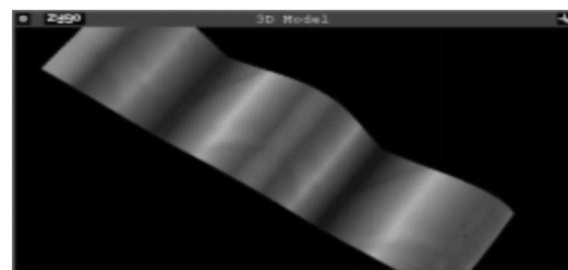

(b) Surface morphology by Zygo interferometer

Fig.7 Photoresist micro-structural and interference morphology

For realizing visible light wave-length transmission, photoresist micro-structure was transfered to quartz substrate surface by ICP–801 plasma etcher machine. Surface topography and deviation value is shown in Fig.8. The roughness of micro-structure arrays surface is 0.035 μm, form error is 29.3 nm.

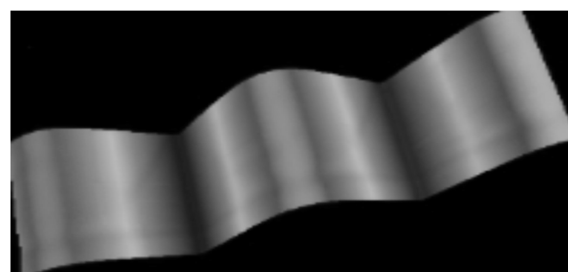

(a) Surface morphology by Zygo interferometer

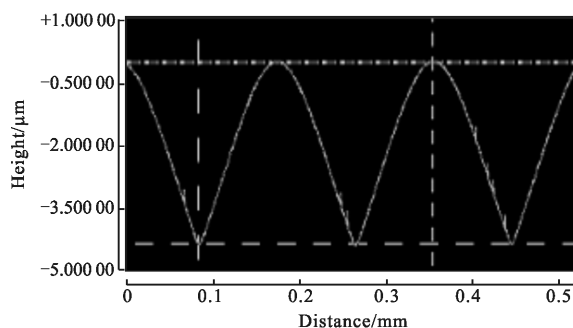

(b) Morphology deviation of cylindrical micro-lens arrays

Fig.8 Interference morphology and deviation

The test result: the transmission of visible light wave-length is 86%, the reflectivity contrastive analysis of 1 064 nm laser total reflectivity is shown in Tab.2, the test result of the different single angle reflectivity is shown in Tab.3.

Tab.2 1 064 nm laser reflectivity contrastive analysis

Incident angle/(°)	0	5	10	15
Simulation power	76.32%	71.94%	75.23%	73.56%
Sample test power	74.71%	73.50%	74.28%	75.10%

Tab.3 Test result of the different single angle reflectivity

Single angle reflectivity		Incident angle/(°)			
		5	10	15	20
Reflection angle /(°)	5	3.4	4.6	3.8	4.4
	10	3.6	2.9	3.8	3.5
	15	4.4	4.2	3.1	3.8
	20	3.6	3.5	4.1	3.8

The experiment result shows that laser total reflectivity t is in agreement with the simulation results, but the reflectivity error exists because of cylindrical optical micro-structure fabrication error. Micro-cylindrical lens arrays can increase reflection light divergence angle, reducing single-directivity reflectivity echo energy shown in Tab.3, it can realize infrared laser protection.

5 Conclusion

Laser protection is a multipurpose technology. The paper designs optical micro-structure made from optical material surface based on drawbacks exist in current optical protection technologies. It scatters to infrared laser with reverse large angle on the premise of lower losses of visible light transmission, which avoids detect ability of vertical reflections as well as equipment and personnel injury caused by specular reflection. It achieves protection to intense laser. Simulation and experiment result shows that the average transmittance of visible light decreases by 7%, but still above 85%. It has little impact on practical application, and we can make it up by fabricating antireflection coating. While stimulating 1 064 nm laser incident cylindrical lens array, the reflectance is over 75% and the divergence angle of target echo is greater than 30°. The maximum intensity area deviates from light source in a certain angle. It reduces the energy of laser single-directivity echo and specular reflection to reach laser protection purpose. We will then carry out experiment verification to design and simulation result with the maturation of experimental conditions. The technology can be popularized other infrared wavelength laser protection, for example 5 μm, 12 μm etc, only cylindrical optical micro-structure is designed for other laser wavelength.

References:

[1] Leng Yanbing, Sun Yanjun. Study on 1×11 Dammann grating with sub-wavelength structure [J]. ***Infrared and Laser Engineering***, 2015, 43(2): 812-817. (in Chinese)

[2] Bai T, Li C Q, Sun J, et al. Covalent modification of graphene oxide with carbazole groups for laser protection[J]. ***Chemistry-A European Journal***, 2015, 21(12): 4622-4627.

[3] Meng X, Lu C, Ni Y, et al. Application and protection of laser technology [J]. ***Infrared and Laser Engineering***, 2005, 2(3): 668-672. (in Chinese)

[4] Zarr R R, Filliben J J. Sensitivity analysis for a guarded-hot-plate apparatus methodology based on orthogonal experiment designs [J]. ***Journal of Testing & Evaluation***, 2016, 44(1): 446-449.

[5] Wang Yonghong, Li Junrui, Sun Jianfei, et al. Frequency domain filtering for phase fringe patterns of digital speckle pattern interferometry [J]. ***Chinese Optics***, 2014, 7 (3): 389-395. (in Chinese)

[6] Hua C, Wang T W, Wang B S, et al. Study of molding preparation technology of laser protective material[J]. ***Optical Technique***, 2005, 18(12): 446-450.

[7] Motomura T, Takahash K, Kasashima Y. Evaluation of SF reactive ion etching performance with a permanent magnet located behind the substrate based on a simple design concept[J]. ***Journal of the Vacuum Society of Japan***, 2016, 59(1): 11-15.

[8] Dong Binchao, Zhang Ge. Fabrication and properties of ultra-lightweight SiC mirror[J]. ***Optics and Precision Engineering***, 2015, 23(8): 2185-2191. (in Chinese)

[9] Fu Huaiyang, Zhou Sizhong, Jiang Kai, et al. Effects of mirror surface roughness on encircled energy for far ultraviolet telescopes [J]. ***Infrared and Laser Engineering***, 2014, 43(8): 2562-2567. (in Chinese)

[10] Kong Ping, Yang Hui, Lin Weimin, et al. Measurement of particle sizes by contrast of dynamic laser speckle [J]. ***Optics and Precision Engineering***, 2014, 22 (10): 2633-2638. (in Chinese)